A compliance control strategy for robot manipulators using a self-controlled stiffness function.

Sang-Rok Oh†, Ho-Chan Kim†, Il Hong Suh‡,
Bum-Jae You†, and Chong Won Lee†

† : Div. of Electronics and Information Technology,
Korea Institute of Science and Technology, Korea

‡ : Dept. of Electronic Engineering,
Hanyang University, Seoul, Korea

Abstract

A compliance control strategy is proposed by using a new type of self-controlled stiffness function, where no explicit wrist force/torque sensor is employed. Specifically, the stiffness gain is given as the exponential function of the error between virtually given desired trajectory and actual trajectory, where virtual desired trajectory is designed to be inside the surface of the object to be compliance-controlled. And, a motion speed scheduling technique is also proposed to avoid serious damages due to lack of environmental knowledge and to minimally maintain the task performances.

It is experimentally shown that the proposed control method is useful for various manipulator motion types such as path following, initial contact with soft impact and force regulation during contact.

1. Introduction

Many a manipulator task requires a series of contact operations. A possible contact motion could be obtained after a phase transition from unconstrained motion to constrained motion. For phase transitions, following motion types can be usually observed: approach, contact motion and possible bouncing if contact failed to be maintained after impact. The robot must successfully manage such motion phases. It is known that a position servo is infinitely stiff and is appropriate when the manipulator is following a trajectory in a free space. It will reject all force disturbances acting on the system. However, when a contact is made between the end-effector and the environment, high stiffness of the end-effector or the environment can make the manipulator be failed to maintain the contact. Small variations in relative positions due to either inaccuracy in position information or errors in position servo can produce undesirable large contact forces. An ideal force servo will exhibit zero stiffness and be able to maintain the desired force. However, force servos can not be useful for trajectory following due to sensitive positional variation even for a small external force disturbance. One way to alleviate these problems is to use a compliant motion controller: some axes of the task coordinate are selected to be force-controlled, and others position-controlled.

Compliant motion control, concerned with the control of a manipulator in contact with its environment, has been discussed extensively during recent years[1]. The well-known approaches include hybrid position/force control [2, 3] and impedance [4] (or stiffness [5]) control. The hybrid position/force control approach is based on an orthogonal decomposition of the task space. In this scheme, forces are controlled to the axes constrained by the environment, while positions are controlled along the axes in which the manipulator is unconstrained and is free to move. However, in the hybrid controller, axes to be constrained and to be unconstrained should be determined before the task begins. Furthermore, if at the instant of impact the desired force magnitude is given to be large, the joint driving torque may suddenly jump. This will result in extreme force overshoot which may be dangerous in many practical situations. As opposed to hybrid control, the control objective of impedance (or stiffness) control is not to track desired position/force trajectories, but to regulate the mechanical impedance of the robot end-effector. Such a control approach has been known to be a unified control one for both the uncon-

0-8186-7108-4/95 $4.00

strained and constrained phases. Here, for a successful constrained motion, a virtual desired trajectory, $X_d(t)$, is given intentionally to be located inside the surface. Since a virtual desired position is located inside the surface, but the end-effector position, X, remains on the surface, the difference $(X_d - X)$ between these two positions multiplied by a manipulator stiffness should result in a contact force. Force regulation is then indirectly achieved by tracking the virtual desired trajectory. Therefore, inaccuracy in the measurement of the output position, if any, may cause a large contact force error. Force tracking is possible only if the environment is near-perfectly modeled.

In this paper, a new type of self-controlled stiffness function is proposed for the compliant motion control of robot manipulators. Specifically, the stiffness gain is given as the exponential function of the error between virtually given desired trajectory and actual trajectory, where virtual desired trajectory is designed to be inside the surface of the object to be compliance-controlled. And, a motion speed scheduling technique is also proposed to avoid serious damages due to lack of environmental knowledge and to minimally maintain the task performances.

2. Dynamics and Stiffness Control

Dynamic behaviors of a nonredundant n degrees-of-freedom manipulator can be modeled as:

$$\tau = M(q)\ddot{q} + H(q,\dot{q}) + G(q), \tag{1}$$

where q, $\dot{q}$ and $\ddot{q}$ are $n \times 1$ vectors of joint positions, velocities, and accelerations, respectively. τ is the $n \times 1$ vector of joint torques supplied by the actuator. $M(q)$ is the $n \times n$ symmetric positive definite inertia matrix and $H(q,\dot{q})$ is the $n \times 1$ vector of centripetal and Coriolis forces. $G(q)$ is the $n \times 1$ vector of gravity.

When a robot contacts its environment, the robot or environment will deform and a reaction force at the end-effector will be produced at each joint. If F is a reaction force at the end-effector in Cartesian coordinate, then the dynamic equation in (1) takes the form,

$$\tau = M(q)\ddot{q} + H(q,\dot{q}) + G(q) + J(q)^T F, \tag{2}$$

where $J(q)$ is the $n \times n$ Jacobian matrix, relating joint velocities to task space velocities.

From the basic stiffness formulation in [5], the joint stiffness matrix K_q is obtained by

$$K_q = J^T K_c J, \tag{3}$$

where K_c denotes a desired $n \times n$ stiffness matrix in Cartesian space. For stiffness control[5], the control input is given by

$$\begin{aligned}\tau &= K_q(q_d - q) + K_d(\dot{q}_d - \dot{q}) + K_f\Big(K_q(q_d - q) \\ &\quad - J^T F\Big) + G(q)\end{aligned} \tag{4}$$

where q_d and $\dot{q}_d$ are $n \times 1$ vectors of desired joint positions and velocities, respectively, K_d is the velocity damping matrix, and K_f is the force feedback gain matrix. Here, it is noted that a wrist force/torque sensor may be necessary to get a closed loop force control system. Unless the sensor is available, diversity of force application may be severely reduced [5]. But, even with such a force sensor, it is usually difficult to obtain force compensation gains because undesired bouncing phenomena are possibly generated at the instant of contact, especially when stiffness of environment is not completely known to the arm, which is often the case in practical assembly processes.

In order to alleviate this problem, we will not employ explicit force control scheme, instead we use only position and velocity information for the compliance control given by

$$\tau = K_q(X, X_d)(q_d - q) + K_d(X, X_d)(\dot{q}_d - \dot{q}) + G(q), \tag{5}$$

where $X_d^T = [x_1^d \ \cdots \ x_n^d]^T$ and $X = [x_1 \ \cdots \ x_n]^T$, respectively, denote desired and actual position vector of robot end effector, and $K_q(X, X_d)$ and $K_d(X, X_d)$ are to be designed as functions of Cartesian positional error, $X_e = X_d - X$.

3. Design of Stiffness Gain Function

If a robot manipulator is to interact effectively with its environment, it must frequently make and break contacts with objects. In this case, the value of the stiffness gain is a compromise between accurate positioning requiring high gain in an unconstrained motion and force tracking requiring low gain in a constrained motion. Even in a constrained motion, the stiffness gain may need to be varied if the stiffness of the environment shows nonlinear behaviors [6, 7]. Specifically, in the cases that the robot end-effector is met by unexpected obstacles and/or that the posture of the object to be handled is changed by unknown disturbances, the stiffness values in Cartesian space are then no longer valid, and hence the stiffness control method using a fixed stiffness gain matrix may not be effective.

In order to cope with such a difficulty, a position error based stiffness gain function is here proposed. It is recalled that no explicit wrist force/torque sensor is employed to get contact information. Instead, the contact is detected by position error. Specifically, if there is an unexpected contact such as a collision with obstacles, a relatively large position error between the actual position and the desired position remains at the instant of the contact. And also, if the desired task is given to perform constrained motions such as deburring, grinding and precision assembly, the contact can be detected from the position error signal by setting the desired trajectory for the robot to virtually move inside the surface [4].

Now, we propose a nonlinear stiffness function in (5) to replace the constant Cartesian stiffness as follows:

$$K_q(X, X_d) = J^T K_c(X, X_d) J$$

where

$$K_c(X, X_d) = \text{diag}\{K_{c1} e^{-k|x_1^d - x_1|},\ K_{c2} e^{-k|x_2^d - x_2|},\ \cdots,\ K_{cn} e^{-k|x_n^d - x_n|}\}, \quad (6)$$

and $K_{c1}, \cdots, K_{cn}$ are chosen to be positive constants with which the asymptotic stability is ensured in unconstrained motions. And the constant k in (6) plays role of determining the decreasing rate.

As a method of determining $K_d(X, X_d)$ in (5), the following simple formula is used:

$$K_d(X, X_d) = \alpha K_q(X, X_d) \quad (7)$$

where $\alpha > 0$ is a scalar scaling coefficient and determines the amount of damping.

Several points can be addressed for the proposed method. Firstly, since each entry of the stiffness gain matrix K_c corresponds to the task coordinate in Cartesian space and decreases during contact only along the corresponding axes, the method can be considered to be self-selective without pre-specifying desired stiffness selection matrix task by task. Secondly, the proposed method can be used for both unconstrained and constrained motion without switching mechanism which often causes undesired vibrational motions of the end effector at the instant of impact. Thirdly, the proposed scheme does not require any explicit measurements of the environmental interaction force. And finally, by determining the velocity damping gain K_d as in (7), we expect that damping of the systems is self-adjusted to prevent force responses from being too sluggish according to the changes of stiffness of the systems.

4. Motion Planning

Surface tracking manipulation tasks, in general, can be completed by simultaneously achieving the following two subgoals:

1) minimum variance path following, and
2) regulation of a contact force of the axes of the end-effector orthogonal to the position or velocity controlled axes for path following.

The desired quantities of motion are not here specified as fixed functions of time. Instead, they are specified as functions of task-related motion quantities. In addition, a virtual desired path to be followed is intentionally given to be inside the surface of the object of which contact forces are to be regulated. Specifically, a real desired joint velocity is determined in accordance with the position error between actual position X and virtual desired position X_d in the Cartesian coordinates. This makes it possible for the motion planner to generate motion commands to be appropriate for the current status of task execution as shown in Fig. 1. The objective of the motion speed scheduling is twofold: one is to avoid serious damages due to the lack of environmental knowledge and the other is to maintain minimum task performances.

Suppose that a desired Cartesian velocity $\dot{X}_d = [\dot{x}_{d1} \ \cdots \ \dot{x}_{dn}]^T$ is given. If the position error $||X_d - X||_\infty (:= \max\{|x_{d1} - x_1| \ \cdots \ |x_{dn} - x_n|\})$ is greater than a prescribed positive constant value, then the real desired speed $\dot{X}_{dreal}$ is obtained by

$$\dot{X}_{dreal} = [\gamma(t)\dot{x}_{d1} \ \cdots \ \gamma(t)\dot{x}_{dn}]^T, \quad (8)$$

and

$$X_{dreal} = [\int \gamma(t)\dot{x}_{d1} dt \ \cdots \ \int \gamma(t)\dot{x}_{dn} dt]^T \quad (9)$$

where $\gamma(t)$ is the scaling factor given by

$$\gamma(t) = \frac{1}{1 + \text{int}(k_1 ||X_d - X||_\infty)} \quad (10)$$

and $\text{int}(x)$ denotes the greatest integer that is smaller than or equal to x and k_1 is a scaling factor.

Furthermore, when the speed is reduced, the scaling coefficient α of the damping matrix K_d in (7) is increased in order to improve transient behaviors of responses.

Remarks

1) Humans perform an unfamiliar task slowly and meticulously since their knowledge on the task

is insufficient and stringent task specifications must be met. By reducing operation speed, for example, they make the task be both tractable and executable despite of insufficient knowledge or limited skills. The required level of task performance is compared with their competence to perform the task. If the task is difficult to execute, its complexity is lowered by reducing operational speed.

2) If the position error $||X_d - X||$ in an unconstrained motion becomes larger than expected, the control gain K_d must be in general readjusted. Judicious judgements must be in these steps, and an effective strategy must be set up to learn the task while executing it satisfactorily. Hence the task complexity is lowered by reducing executing speed and damping matrix K_d is readjusted using α in (7).

5. Experimental Verifications

For experimental verifications of the proposed stiffness control algorithms, our own developed two-link direct drive robot manipulator is used as shown in Fig. 2.

The physical parameters of the robot are given in Table 1.

5.1. Experimental Hardwares

The configuration of the real-time robot control system is shown in Fig. 3, where each joint has a resolver and a tachometer to measure the joint position and the joint velocity, respectively. The control algorithms are coded by a C language, download into the single board computer MVME-147 through the data transition module MVME-712, and performed with helps of the real-time O.S. VxWorks [8]. The analog signals are sampled and digitized by the A/D converter board, MACRO-6780 and the command torque signals are transferred to actuator drives by the D/A converter board, MACRO-6781. The pulse signals from resolver signal processing units are counted to measure positions by using the pulse counter module, HIME-607A and the counted value is then transmitted to MVME-147 at every sampling time. The control signal update and the data feedback for each joint are executed at every 5[msec] with the aids of a real-time O.S., VxWorks.

5.2. Experimental Results

To test the effectiveness of the proposed stiffness control algorithm, a simple task is chosen: the virtual desired position X_d is given as a circle in the workspace. And a rigid barrier is placed in the workspace in such a way that its flat front surface are to be intersected with the circle. This task is provided for a comprehensive test of the universal ability of the proposed stiffness controller to handle the following cases: path following ability in a free space, ability of regulation of the interaction forces during constrained motions, and ability of smooth impact force control during the transitions between path control and force regulation phases.

During free motion phase, the force is zero and the path of the end-effector should be an arc of a circle. Upon contacting the barrier, the end-point should smoothly land on the barrier surface along a chord of the circle defined by the surface of the barrier. At the moment of contact with the barrier, there may be an impulsive force due to the collision of the end-point inertia with the rigid surface, but immediately such an impulsive force should be made to disappear. Then, since the desired position X_d becomes located inside the surface, but the current end-effector position, X, remains on the surface, a relatively large difference between X_d and X will be detected and thus can be known that compliance control is required. Here, force/torque sensor is used only for measurements of interaction force to evaluate the proposed algorithm.

The experimental results are shown in Fig. 4 and Fig. 5. For cases of constant and proposed position error dependent stiffness, both systems show stable actions throughout all phases of the task. Especially similar path following performances are obtained. A careful observation on two path following performances lets us know that during the unconstrained motion phase of the task, the end-effector trajectory by the proposed control scheme is getting closer to the desired trajectory than that by the constant stiffness control. However, the interaction forces in both cases ,during the constrained motion phase of the task, are shown to be quite different. From Fig. 4, one can observe that if the constant stiffness control is used, an interaction force increases as a position error $||X_d - X||$ increases and is sensitive to disturbance. However, as shown in Fig. 5, interaction forces by the proposed control algorithm becomes relatively small and is insensitive to disturbances.

6. Concluding Remarks

A self-controlled stiffness function was proposed for controlling various types of manipulator motions such as path following, initial contact with soft im-

pact and force regulation during contact without both any switching mechanisms and any knowledge on the environment in constrained and unconstrained spaces. The proposed method was experimentally shown to work satisfactorily for a compliance control task, where our own developed two-link manipulator was employed. As one of our future works, mathematical stability analysis is to be investigated.

References

[1] M. W. Spong and M. Vidyasgar, *Robot dynamics and control.* John Wiley & Sons, Inc, 1989.

[2] M. H. Raibert and J. J. Craig, "Hybrid position/force control of manipulators," *ASME J. Dyn. syst. Meas. Contr.*, vol. 102, no. 1, pp. 126–133, 1981.

[3] R. Volpe and P. Khosla, "A theoretical and experimental investigation of explicit force control strategies for manipulators," *IEEE Trans. Automat. Contr.*, vol. 38, no. 11, pp. 1634–1650, 1993.

[4] N. Hogan, "Impedance control: An approach to manipulation, Part 1: Theory; Part 2: Implementation; Part 3: Applications," *ASME J. Dyn. syst. Meas. Contr.*, vol. 107, no. 1, pp. 1–24, 1985.

[5] J. K. Salibury, "Active stiffness control of manipulator in Cartesian coordinates," in *Proc. IEEE 19th Conf. on Decision and Control*, pp. 95–100, 1980.

[6] I. H. Suh, K. S. Eom, H. J. Yeo, B. H. Kang, S. R. Oh, and B. H. Lee, "Explicit fuzzy force control of industrial manipulators with position servo drives," in *Proc. IEEE/RSJ Int. Conf. Intelligent Robots and Systems*, (Munich), pp. 657–664, September 1994.

[7] I. H. Suh, K. S. Eom, H. J. Yeo, and S. R. Oh, "Adaptive fuzzy force control of industrial manipulators with position servos," submitted to *IEEE/RSJ Int. Conf. Intelligent Robots and Systems*, 1995.

[8] V. Manual, *Real-Time Operating System.* Ready System Co., 1992.

Table 1. Physical parameters of the robot arm.

	Link 1	Link 2
Mass of link	22 Kg	12 Kg
Length	0.395 m	0.365 m
Mass of motor	73 Kg	13 Kg
Rotor inertia	1.07 $Kgfm^2$	0.031 $Kgfm^2$
Friction coefficient	1.0 $kgfm$	0.01 $Kgfm$

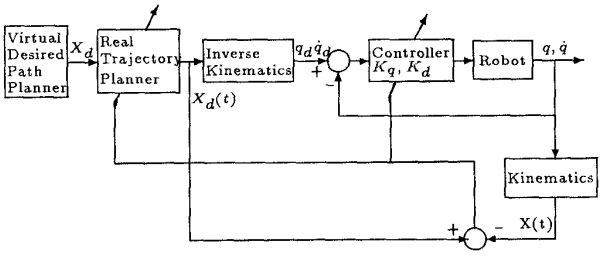

Figure 1: Self-controlled stiffness control strategy.

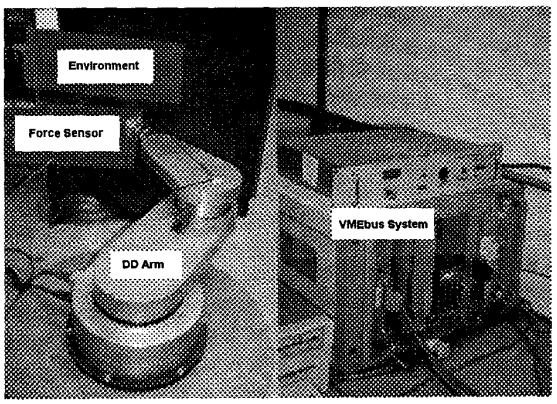

Figure 2: Our own developed two-linked direct drive robot arm performing the task and its control system.

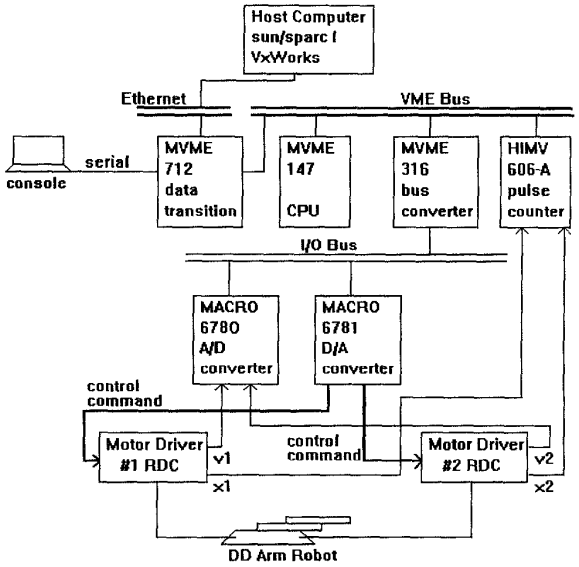

Figure 3: The hardware configuration of the controller for two-links robot arm control system.

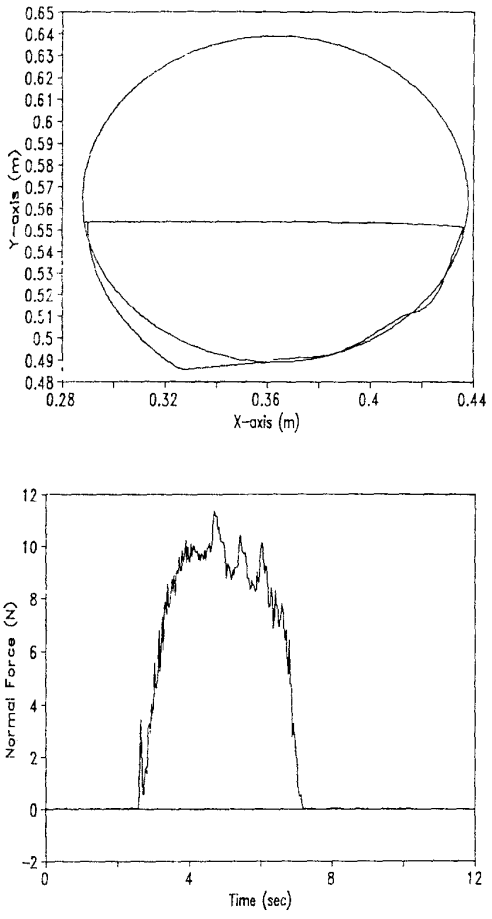

Figure 4: Actual performance of the experimental apparatus on the task when self-learning stiffness was not used. The path of the end-point is shown on the top. The time history of interaction force is shown on the bottom.

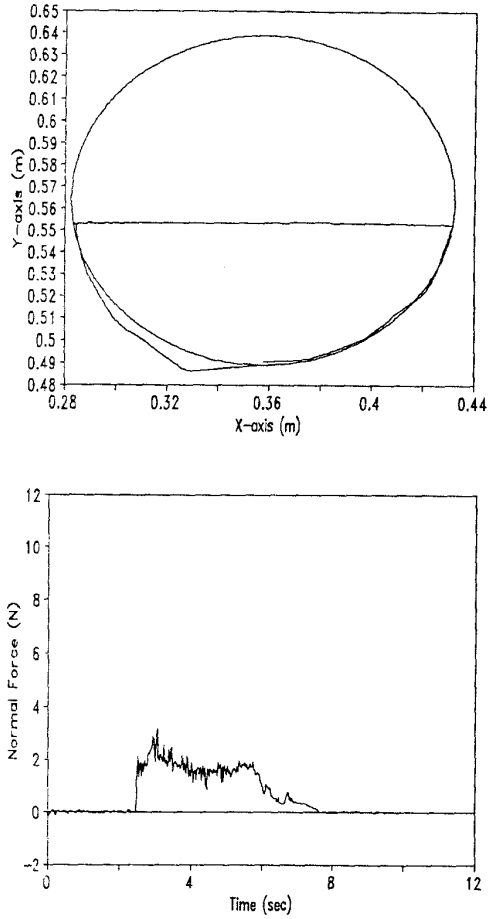

Figure 5: Actual performance of the experimental apparatus on the task when self-learning stiffness was used. The path of the end-point is shown on the top. The time history of interaction force is shown on the bottom.